Inorg. Chem. **2007**, *46*, 93–102

Synthesis and Characterization of Silyldichloramines, Their Reactions with F^- Ions, Instability of N_2Cl_2 and NCl_2^-, and Formation of NCl_3

Stefan Schneider,*[,†,§] Michael Gerken,[†,¶] Ralf Haiges,[†] Thorsten Schroer,[†,§] Jerry A. Boatz,[‡] David A. Dixon,[¥] Daniel J. Grant,[¥] and Karl O. Christe*[,†]

Loker Hydrocarbon Research Institute and Department of Chemistry, University of Southern California, Los Angeles, California 90089, Air Force Research Laboratory, Edwards Air Force Base, California 93524, and Department of Chemistry, University of Alabama, Tuscaloosa, Alabama 35487-0336

Received May 24, 2006

Only two silyldichloramines, $(C_6H_5)_3SiNCl_2$ and $(CH_3)_3SiNCl_2$, have been reported in the literature. The synthesis of the former was successfully repeated, and its structure was established by single-crystal X-ray diffraction and vibrational spectroscopy. Attempts to prepare $(CH_3)_3SiNCl_2$ were unsuccessful; however, a new trialkylsilyldichloramine, *t*-$BuMe_2Si–NCl_2$, was prepared and characterized by Raman and multinuclear NMR spectroscopy. The reaction of *t*-$BuMe_2SiNCl_2$ with $(CH_3)_4NF$ in CHF_3 solution at −78 °C, followed by removal of all volatile products at −30 °C, produced the expected *t*-$BuMe_2SiF$ byproduct and a white solid consisting of NCl_3 absorbed on Me_4NCl. The NCl_3 could be reversibly desorbed from the substrate and was identified as a neat liquid at room temperature by Raman spectroscopy. The observed final reaction products are consistent with the formation of an unstable $N(CH_3)_4^+NCl_2^-$ intermediate which decomposes to $N(CH_3)_4^+Cl^-$ and NCl molecules which can dimerize to N_2Cl_2. Theoretical calculations confirm that NCl_2^- can readily lose Cl^- and that N_2Cl_2 also possesses a low barrier toward loss of N_2 to give chlorine atoms and, thus, can account for the formation of NCl_3.

Introduction

Chloramines are important intermediates in the industrial production of hydrazine by the Raschig process and hold potential as precursors for the synthesis of azidamines. However, neat chloramines are highly unstable and often can decompose explosively. Therefore, relatively little is known about these compounds. Chloramine chemistry had its ominous beginning in 1811 when Dulong lost three fingers and an eye during the discovery of NCl_3. Almost a century later in 1908, a second nitrogen chloride, chlorine azide, was observed by Raschig when he added acetic acid to equimolecular amounts of sodium azide and sodium hypochlorite in aqueous solution. Another 12 years went past before Marckwand and Wille added NH_2Cl to the nitrogen chloride family, followed by the synthesis of $NHCl_2$ in 1929 by Chapin.[1,2] It is noteworthy that almost another half a century went by until in 1977 and 1990 the first nitrogen chloride ions, $ONCl_2^+$ and NCl_4^+, were reported,[3,4] but so far the synthesis of neither one has been confirmed.

Very recently, we reported the syntheses and characterization of $NH_3Cl^+M^-$ salts ($M = BF_4$, AsF_6, SbF_6) in which the explosiveness and thermal instability of the parent molecule NH_2Cl were circumvented using an organosilicon derivative, $(Me_3Si)_2NCl$, as the starting material.[5] Generally, covalent R_3Si-X bonds can be readily cleaved by strong acids and nucleophiles, such as fluoride ions. In the case of $(Me_3Si)_2NCl$, the silicon nitrogen bond was cleaved by

* To whom correspondence should be addressed. E-mail: kchriste@usc.edu (K.O.C.); stefan.schneider@edwards.af.mil (S.S.).
† University of Southern California.
‡ Air Force Research Laboratory.
¥ University of Alabama.
§ Present address: Air Force Research Laboratory, Edwards AFB, California 93524.
¶ Present address: Department of Chemistry and Biochemistry, The University of Lethbridge, Alberta, T1K 3M4, Canada.

(1) Holleman, A. F.; Wiberg, N. *Inorganic Chemistry;* Academic Press: San Diego, CA, 2001.
(2) Greenwood, N. N.; Earnshaw, A. *Chemistry of the Elements*, 2nd ed.; Butterworth-Heinemann: Oxford, U.K., 1998.
(3) (a) Dehnicke, K.; Aeissen, H; Koelmel, M.; Straehle, J. *Angew. Chem., Int. Ed. Engl.* **1977**, *16*, 545. (b) Minkwitz, R.; Bernstein, D.; Sawodny, W.; Haertner, H. *Z. Anorg. Allg. Chem.* **1990**, *580*, 109.
(4) Minkwitz, R.; Bernstein, D.; Sawodny, W. *Angew. Chem., Int. Ed. Engl.* **1990**, *29*, 181.
(5) Schneider, S.; Haiges, R.; Schroer, T.; Boatz, J.; Christe, K. O. *Angew. Chem.* **2004**, *43*, 5213.

10.1021/ic0609103 CCC: $37.00
Published on Web 12/06/2006

anhydrous HF in the presence of Lewis acids, resulting in the formation of the desired NH_3Cl^+ salts (eq 1).

$$(R_3Si)_2NCl + 3\,HF + MF_5 \rightarrow NH_3Cl^+MF_6^- + 2R_3SiF \quad (1)$$

In this paper, we describe a modification of this approach which has the potential to generate nitrogen chloride anions instead of cations using the strongly basic fluoride anion in place of the HF/MF_5 superacid system as the cleaving agent (eq 2). Although the chlorination of amine complexes of

$$R_3SiNCl_2 + Me_4N^+F^- \rightarrow Me_4N^+NCl_2^- + R_3SiF \quad (2)$$

platinum (IV+) affords covalently bonded NCl_2 ligands[6] and numerous free pseudo-halide amide anions, NX_2^- (X = SO_2F,[7] SO_2CF_3,[8] SO_2Cl,[9] CF_3,[10] SF_5,[11] TeF_5,[12] CN[13]), are known, the free NCl_2^- anion is unknown.

Surprisingly, little was known about the required triorganylsilydichloramines starting materials. To the best of our knowledge, only two examples of this class of compounds, triphenylsilyldichloramine[14] and trimethylsilyldichloramine,[15] have previously been reported. Therefore, the synthesis of these compounds was reexamined.

Experimental Section

Caution: *Neat chloramines are highly unstable and often can decompose explosively. They should be handled on a small scale with appropriate safety precautions. The handling of neat NCl_3, especially, has led to serious injuries!*

Materials and Apparatus. Reactions were carried out in Teflon−FEP ampules that contained Teflon-coated magnetic stirring bars and were closed by stainless steel valves. The valves were attached to the ampules through stainless steel T-fittings. The valve was attached to the horizontal part of the T, and the top end of the T was closed by a removable stainless steal cap to allow the addition of solids or liquids to the ampule under dry nitrogen conditions. Volatile materials were handled on a Pyrex glass vacuum line equipped with grease-free Kontes glass−Teflon valves. Nonvolatile solids were handled in the dry nitrogen atmosphere of a glove box. Infrared spectra were recorded on a Midac M Series FT-IR spectrometer using dry powders pressed between AgCl windows in an Econo press (Barnes Engineering Co.). Raman spectra were recorded in the range of 4000−80 cm^{-1} on a Bruker Equinox 55 FT-RA 106/S spectrometer using a Nd:YAG laser at 1064 nm. Pyrex melting-point capillaries, glass NMR tubes, or 9 mm Teflon−FEP tubes were used as sample containers. Nuclear magnetic resonance spectra were recorded unlocked on a Bruker AMX 500 NMR spectrometer at room temperature. The ^1H, ^{13}C, and ^{29}Si (^{14}N) NMR spectra were referenced to external samples of neat TMS, (neat nitromethane).

The Ph_3SiNCl_2 was prepared using the literature method.[14] Diethylether was dried over sodium. NH_3 (Aldrich, anhydrous, 99.99%), CF_3H (Matheson Co.), Ph_3SiNH_2 (Aldrich, 97%), *tert*-$BuMe_2SiCl$ (Aldrich, 97%), and *tert*-BuOCl (TCI, 98%) were used without further purification. Tetramethylammonium fluoride tetrahydrate (Aldrich, 98%) was dehydrated by a literature method.[16]

Crystal Structure Determination of Ph_3SiNCl_2. (a) Collection and Reduction of X-ray Data. The crystal used in this study had dimensions of 0.155 × 0.152 × 0.106 mm^3. X-ray diffraction data were collected using a Bruker 3-circle platform diffractometer, equipped with a SMART APEX CCD (charge-coupled device) detector with the χ axis fixed at 54.74° (using the program SMART[17]), and using Mo Kα radiation (λ = 0.71073 Å) from a fine-focus tube. The diffractometer was equipped with a cryo-cooler from CRYO Industries for low-temperature data collection using controlled liquid nitrogen boil off. Cell constants were determined from 60 ten-second frames at 130 K. A complete hemisphere of data was collected up to a resolution of 0.75 Å. Processing was carried out using the program SAINT,[18] which applied Lorentz and polarization correction to three-dimensionally integrated diffraction spots. The program SADABS[19] was used for the scaling of diffraction data, the application of a decay correction, and an empirical absorption correction based on redundant reflections.

(b) Solution and Refinement of the Structure. All data were processed using the SHELXTL package (version 5.1)[20] for structure determination, refinement, and molecular graphics. The XPREP program was used to confirm the unit cell dimensions and the crystal lattice. The structure was solved by the direct method. Successive difference Fourier syntheses revealed all atoms. The structure was refined by the least-squares method on F^2. All atoms except hydrogen were refined anisotropically. For the anisotropic displacement parameters, U(eq) is defined as one-third of the trace of the orthogonalized U^{ij} tensor.

CCDC 253436 contains the supplementary crystallographic data for this paper. These data can be obtained free of charge via www.ccdc.cam.ac.uk/data_request/cif, by emailing data_request@ccdc.cam.ac.uk, or by contacting The Cambridge Crystallographic Data Centre, 12 Union Road, Cambridge CB2 1EZ, U.K. (fax +44 1223 336033).

Raman Data for Ph_3SiNCl_2 (relative intensity): 3174 (3), 3134 (6), 3054 (100), 2998 (3), 2978 (3), 2958 (4), 2894 (1), 2851 (1), 2820 (<0.5), 2773 (<0.5), 2685 (<0.5), 2596 (1), 2524 (1), 2424 (1), 1589 (42), 1568 (9), 1482 (1), 1429 (2), 1336 (2), 1309 (1), 1188 (8), 1160 (11), 1115 (1), 1102 (11), 1071 (1), 1028 (28), 999 (87), 986 (1), 923 (1), 858 (2), 828 (14), 745 (1), 715 (3), 688 (16), 678 (2), 619 (6), 513 (11), 446 (12), 437 (4), 399 (<0.5), 391 (<0.5), 329 (10), 308 (23), 250 (3), 238 (17), 220 (6), 212 (2), 179 (1), 169 (32), 121 (3), 95 (83) cm^{-1}.

(6) (a) Kukushkin, Y. N. *Zh. Neorg. Khim.* **1957**, *2*, 2371. (b) Kukushkin, Y. N. *Zh. Neorg. Khim.* **1959**, *4*, 2460. (c) Kukushkin, Y. N. *Zh. Neorg. Khim.* **1960**, *5*, 1943. (c) Kukushkin, Y. N. *Zh. Neorg. Khim.* **1961**, *6*, 1762. (d) Kukushkin, Y. N. *Zh. Neorg. Khim.* **1962**, *7*, 769. (e) Kukushkin, Y. N. *Zh. Neorg. Khim.* **1962**, *7*, 1795. (f) Kukushkin, Y. N. *Zh. Neorg. Khim.* **1965**, *10*, 601. (g) Varshavskii, Y. S.; Kukushkin, Y. N. *Zh. Neorg. Khim.* **1965**, *10*, 1332.

(7) Ruff, J. K. *Inorg. Chem.* **1965**, *4*, 1446.

(8) Foropoulos, J., Jr.; DesMarteau, D. *Inorg. Chem.* **1984**, *23*, 3720.

(9) Becke-Goering, M.; Hormuth, B. *Z. Anorg. Allg. Chem.* **1969**, *369*, 105.

(10) Minkwitz, R; Liedtke, A. *Inorg. Chem.* **1989**, *28*, 1627.

(11) (a) Hoefer, R.; Glemser, O. *Z. Naturforsch.* **1975**, *30b*, 458. (b) Waterfeld, A.; Mews, R. *Angew. Chem., Int. Ed. Engl*. **1982**, *21*, 354.

(12) Thrasher, J. S.; Seppelt, K. *Angew. Chem., Int. Ed. Engl*. **1983**, *22*, 789.

(13) (a) Starynowicz, P. *Acta Crystallogr*. **1991**, *C47*, 2198. (b) Bu, X.; Coppens, P. *Acta Crystallogr.* **1992**, *C48*, 1560.

(14) Wiberg, N.; Raschig, F. *J. Organomet. Chem.* **1967**, *10*, 15.

(15) Wiberg, N.; Uhlenbrock, W. *Chem. Ber.* **1971**, *104*, 2643.

(16) Christe, K. O.; Wilson, W. W.; Wilson, R. D.; Bau, R.; Feng, J. *J. Am. Chem. Soc.* **1990**, *112*, 7619.

(17) *SMART, Software for the CCD Detector System*, version 5.625; Bruker AXS: Madison, WI, 2001.

(18) *SAINT, Software for the CCD Detector System*, version 6.22; Bruker AXS: Madison, WI, 2001.

(19) *SADABS, Program for Absorption Correction for Area Detectors*, version 2.03; Bruker AXS: Madison, WI, 2001.

(20) *SHELXTL, Program Library for Structure Solution and Molecular Graphics*, version 6.22 for Windows NT; Bruker AXS: Madison, WI, 2000.

Preparation of *t*-BuMe$_2$SiNH$_2$. In a variation of the published literature methods,[21,22] a solution of 15.79 g (119.48 mmole) of *t*-BuMe$_2$SiCl in ~50 mL diethylether was pressurized in a 200 mL flask with excess anhydrous ammonia and stirred overnight at room temperature to ensure the completion of the reaction. The reaction mixture was then cooled to −196 °C, and the volatile products, solvent, and *t*-BuMe$_2$SiNH$_2$, were separated by fractional condensation by pumping them, upon warming up to room temperature, through two cold traps kept at −24 (CCl_4 slush bath) and −196 °C. A glass-wool plug was placed inside the connector between the reaction vessel and the −24 °C cold-trap, ensuring that none of the NH_4Cl byproduct was swept from the reactor into the cold trap. The −24 °C trap contained the desired *t*-BuMe$_2$SiNH$_2$ as a white, crystalline solid in better than 90% yield. The purity of the *t*-BuMe$_2$SiNH$_2$ was verified by Raman and NMR spectroscopy.

Preparation of *t*-BuMe$_2$SiNCl$_2$. By analogy with the method published for the preparation of Ph_3SiNCl_2,[14] *t*-BuOCl (15.914 g, 146.58 mmol) was added dropwise in the dark to an ice-cooled stirred solution of *t*-BuMe$_2$SiNH$_2$ (8.776 g, 66.38 mmol) in dry diethylether. The solution turned immediately yellow, but no precipitate was formed, as in the case of Ph_3SiNCl_2, because, contrary to Ph_3SiNCl_2, *t*-BuMe$_2$SiNCl$_2$ is soluble in diethylether. The solvent was pumped off between −78 and −30 °C. Because of the volatilities of *t*-BuMe$_2$SiNCl$_2$ and *t*-BuOH, the byproduct formed in the reaction, are similar, further pumping of the residual *t*-BuMe$_2$SiNCl$_2$/*t*-BuOH mixture at RT (room temperature) was required for the isolation of pure, highly viscous *t*-BuMe$_2$SiNCl$_2$ (13.18 mmol, ~20%). Most of the product was lost during this procedure, indicating that *t*-BuOH has only a slightly higher volatility than *t*-BuMe$_2$SiNCl$_2$. The isolated yield of *t*-BuMe$_2$SiNCl$_2$ could certainly be improved by the use of better separation techniques. The purity of the product was continuously monitored by Raman and NMR spectroscopy.

Raman data for *t*-BuMe$_2$SiNCl$_2$ (relative intensity): 2964 (57), 2931 (64), 2905 (100), 2864 (68), 2781 (10), 2713 (7), 1464 (14), 1445 (12), 1409 (5), 1401 (5), 1365 (3), 1256 (3), 1213 (14), 1184 (5), 1013 (3), 1005 (3), 941 (7), 832 (9), 819 (16), 779 (11), 745 (3), 676 (22), 578 (26), 463 (27), 438 (17), 399 (7), 365 (7), 354 (9), 332 (19), 305 (17), 218 (24), 168 (12), 148 (11), 123 (11), 83 (15) cm^{-1}.

Reaction of *t*-BuMe$_2$SiNCl$_2$ with Me$_4$NF and Generation of NCl$_3$. In a typical experiment, *t*-BuMe$_2$SiNCl$_2$ (0.607 g, 3.03 mmol) was loaded with a pipet into one of the above-described Teflon−FEP ampules. To exclude moisture, this operation was carried out in dry nitrogen streams, which were passed through the *t*-BuMe$_2$SiNCl$_2$ storage vessel and the Teflon ampule. The ampule was then cooled to −196 °C and evacuated, and a layer of CF_3H was condensed into the mixture at this temperature on the vacuum line. An equimolar amount of Me_4NF was added to the frozen mixture in a stream of dry nitrogen, followed by an additional layer of CF_3H. The mixture was then warmed to −78 °C and vigorously stirred. The reaction was stopped when the yellow color of *t*-BuMe$_2$SiNCl$_2$ had disappeared. The solvent CF_3H and the generated N_2 were pumped off at −78 °C, and a stoichiometric amount of *t*-BuMe$_2$SiF was removed between −30 and −20 °C. At this temperature, the solid residue consisted only of NCl_3 absorbed on Me_4NCl. Warming of the solid to room-temperature resulted in the slow reversible release of NCl_3.

Computational Approach. The calculations were done at the CCSD(T) level, except as described below. Only the spherical components (5-*d*, 7-*f*, and 9-*g*) of the Cartesian basis functions were used. All of the current work was performed with the MOLPRO suite of programs.[23] The open-shell CCSD(T) calculations for the atoms were carried out at the R/UCCSD(T) level. In this approach, a restricted open-shell Hartree−Fock (ROHF) calculation was initially performed, and the spin constraint was relaxed in the coupled cluster calculation.[24−26] All of the calculations were done on the 144 processor Cray XD-1 computer system at the Alabama Supercomputer Center.

The geometries were optimized numerically at the frozen core CCSD(T) level with the aug-cc-pVDZ and aug-cc-pVTZ correlation-consistent basis sets (we abbreviate the names to aVnZ).[27] It has recently been found that tight d functions are necessary for the calculation of accurate atomization energies for second row elements,[28] so additional tight d functions were included in our final energy calculations. The CCSD(T)/aug-cc-pVDZ geometries were used in the single point CCSD(T)/aug-cc-pV(D+d)Z calculations, and the CCSD(T)/aug-cc-pVTZ geometries were used in the single point CCSD(T)/aug-cc-pV(T+d)Z and CCSD(T)/aug-cc-pV(Q+d)Z calculations. Bond distances, harmonic frequencies, and anharmonicity constants for the diatomic NCl ($^3\Sigma$) were obtained from a fifth-order fit of the potential energy surface at the CCSD(T)/aug-cc-pV(Q+d)Z level. The vibrational frequencies for NCl_2^- were calculated at the CCSD(T)/aug-cc-pVTZ level.[29] The CCSD(T) total energies were extrapolated to the CBS limit by using a mixed exponential/Gaussian function of the form

$$E(n) = E_{CBS} + A \exp[-(n-1)] + B \exp[-(n-1)^2]$$

with $n = 2$ (DZ), 3 (TZ), and 4 (QZ), as first proposed by Peterson et al.[30] This extrapolation method has been shown to yield atomization energies in the closest agreement with experiment (by a small amount) as compared to other extrapolation approaches up through $n = 4$.

Core-valence corrections, ΔE_{CV}, were obtained at the CCSD(T)/cc-pwCVTZ level of theory.[31] Scalar relativistic corrections (ΔE_{SR}), which account for changes in the relativistic contributions to the total energies of the molecule and the constituent atoms, were included at the CI-SD (configuration interaction singles and doubles) level of theory using the cc-pVTZ basis set. ΔE_{SR} is taken as the sum of the mass−velocity and one-electron Darwin (MVD) terms in the Breit−Pauli Hamiltonian.[32]

(21) Kraus, C. A.; Rosen, R. *J. Am. Chem. Soc.* **1925**, *47*, 2739.
(22) Dugat, D.; Just, G.; Sahoo, S. *Can. J. Chem.* **1987**, *65*, 88.
(23) Werner, H. J.; Knowles, P. J.; Amos, R. D.; Bernhardsson, A.; Berning, A.; Celani, P.; Cooper, D. L.; Deegan, M. J. O.; Dobbyn, A. J.; Eckert, F.; Hampel, C.; Hetzer, G.; Korona, T.; Lindh, R.; Lloyd, A. W.; McNicholas, S. J.; Manby, F. R.; Meyer, W.; Mura, M. E.; Nicklass, A.; Palmieri, P.; Pitzer, R. M.; Rauhut, G.; Schütz, M.; Stoll, H.; Stone, A. J.; Tarroni, R.; Thorsteinsson, T. *MOLPRO-2002, A Package of Initio Programs* ; Universität Stuttgart: Stuttgart, Germany; University of Birmingham: Birmingham, U.K., 2002.
(24) Rittby, M.; Bartlett, R. J. *J. Phys. Chem.* **1988**, *92*, 3033.
(25) Knowles, P. J.; Hampel, C.; Werner, H. J. *J. Chem. Phys.* **1994**, *99*, 5219.
(26) Deegan, M. J. O.; Knowles, P. J. *Chem. Phys. Lett.* **1994**, *227*, 321.
(27) (a) Dunning, T. H., Jr. *J. Chem. Phys.* **1989**, *90*, 1007. (b) Kendall, R. A.; Dunning, T. H., Jr.; Harrison, R. J. *J. Chem. Phys.* **1992**, *96*, 6796.
(28) Dunning, T. H., Jr.; Peterson, K. A.; Wilson, A. K. *J. Chem. Phys.* **2001**, *114*, 9244.
(29) (a) Møller, C.; Plesset, M. S. *Phys. Rev.* **1934**, *46*, 618. (b) Pople, J. A.; Binkley, J. S.; Seeger, R. *Int. J. Quantum Chem. Symp.* **1976**, *10*, 1.
(30) Peterson, K. A.; Woon, D. E.; Dunning, T. H., Jr. *J. Chem. Phys.* **1994**, *100*, 7410.
(31) (a) Peterson, K. A.; Dunning, T. H., Jr. *J. Chem. Phys.* **2002**, *117*, 10548. (b) Woon, D. E.; Dunning, T. H., Jr. *J. Chem. Phys.* **1993**, *98*, 1358.
(32) Davidson, E. R.; Ishikawa, Y.; Malli, G. L. *Chem. Phys. Lett.* **1981**, *84*, 226.

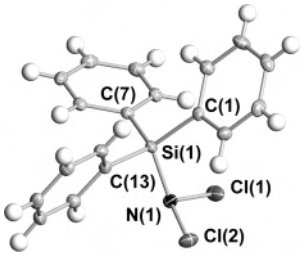

Figure 1. Structure of the Ph_3SiNCl_2 molecule. Thermal ellipsoids are shown at the 50% probability level.

Table 1. Crystal Data for Ph_3SiNCl_2

chemical formula	$C_{18}H_{15}C_{l2}NSi$
fw	344.30
T (K)	85(2)
space group	$P\bar{1}$, triclinic
a (Å)	9.073(2)
b (Å)	9.797(2)
c (Å)	10.1333(2)
α (deg)	107.983(4)
β (deg)	102.954(4)
γ (deg)	96.174(4)
V (Å^3)	819.6(3)
Z	2
ρ_{calcd} (g cm^{-3})	1.395
μ (mm^{-1})	0.464
R1,[a] wR2[b] [$I > 2\sigma(I)$]	0.0391, 0.0939
R1,[a] wR2[b] (all data)	0.0453, 0.0973

[a] $R1 = (\sum(F_0 - F_c)/F_0)$. [b] $wR2 = [\sum(w(F_0 - F_c)^2)w/F_0^2)]^{1/2}$.

By combining our computed ΣD_0 (total atomization energies) values with the known heats of formation at 0 K for the elements $\Delta H_f^0(N) = 112.53 \pm 0.02$ kcal mol^{-1}and $\Delta H_f^0(Cl) = 28.59$ kcal mol^{-1}, we can derive ΔH_f^0 values for the molecules under study in the gas phase. We obtain heats of formation at 298 K by following the procedures outlined by Curtiss et. al.[33]

Results and Discussion

Synthesis and Properties of Ph_3SiNCl_2. Of the two previously reported triorganylsilyldichloramines, triphenylsilyldichloramine[14] and trimethylsilyldichloramine,[15] only the latter would be volatile enough to allow easy low-temperature product separation from other nonvolatile reaction products. However, our efforts were unsuccessful to repeat the previously described[14] preparation of this compound. Instead of the required unstable $(CH_3)_3SiNH_2$ intermediate, only $[(CH_3)_3Si]_2NH$ was formed which, upon chlorination, produced $[(CH_3)_3Si]_2NCl$.[5] Therefore, the preparation of the triphenylsilyldichloramine was reexamined (eq 3).

$$Ph_3SiNH_2 + 2t\text{-BuOCl} \rightarrow Ph_3SiNCl_2 + 2t\text{-BuOH} \quad (3)$$

The compound was successfully prepared and characterized by its X-ray crystal structure (Figure 1, Tables 1−3) and Raman spectrum (Figure 2) because previously only its melting point and proton NMR spectrum had been reported.[14]

Ph_3SiNCl_2 crystallizes in the triclinic space group $P\bar{1}$. The most interesting part of the molecule (Figure 1) is the nitrogen environment, which is close to tetrahedral with Cl−N−Cl and Cl−N−Si bond angles of 108.4(1) and 112.1(1)°, respectively. The increased repulsion from the bulky phenyl groups and the sterically active, free valence-electron pair on the nitrogen atom are responsible for the relatively long silicon−nitrogen distance of 181.2(2) pm. The N−Cl bond lengths of 173.8(2) and 175.4(2) pm are similar to those found in $CH_3C_6H_4SO_2NCl_2$ and $CH_3SO_2NCl_2$.[34,35] The bond distances and angels of the triphenylsilyl group are as expected.

No attempt was made to completely assign the Raman spectrum because of its complexity caused by the triphenylsilyl group. However, a comparison between the Raman spectra of the Ph_3SiNH_2 starting material and the Ph_3SiNCl_2

Table 2. Selected Bond Lengths (Å) and Angles (deg) for Ph_3SiNCl_2

Si(1)−N(1)	181.3(2)	N(1)−Si(1)−C(1)	100.53(8)
Si(1)−C	185.7(2)−186.2(2)	N(1)−Si(1)−C(13)	104.77(8)
N(1)−Cl(1)	173.8(2)	N(1)−Si(1)−C(7)	113.84(8)
N(1)−Cl(2)	175.4(2)	C(7)−Si(1)−C(13)	111.33(8)
		C(7)−Si(1)−C(1)	113.42(8)
		C(1)−Si(1)−C(13)	112.22(8)
		Cl(1)−N(1)−Cl(2)	108.43(9)
		Cl(1)−N(1)−Si(1)	112.07(9)
		Cl(2)−N(1)−Si(1)	112.10(9)

Table 3. Atomic Coordinates ($\times 10^4$) and Equivalent Isotropic Displacement Parameters ($\times 10^3$ Å^2) for Ph_3SiNCl_2

	x	y	Z	U(eq)[a]
Si(1)	3696(1)	1371(1)	3032(1)	14(1)
N(1)	2559(2)	2103(2)	1794(2)	19(1)
C(1)	3041(2)	−621(2)	2029(2)	16(1)
C(2)	4077(2)	−1586(2)	1894(2)	18(1)
C(3)	3562(3)	−3067(2)	1114(2)	22(1)
C(4)	2008(2)	−3607(2)	453(2)	22(1)
C(5)	958(2)	−2671(2)	575(2)	21(1)
C(6)	1466(2)	−1197(2)	1355(2)	19(1)
C(7)	5810(2)	1992(2)	3440(2)	15(1)
C(8)	6570(2)	1792(2)	2350(2)	21(1)
C(9)	8158(2)	2237(2)	2685(2)	23(1)
C(10)	9017(2)	2895(2)	4106(2)	23(1)
C(11)	8295(2)	3094(2)	5198(2)	23(1)
C(12)	6708(2)	2639(2)	4869(2)	19(1)
C(13)	3020(2)	1976(2)	4689(2)	15(1)
C(14)	2201(2)	937(2)	5080(2)	17(1)
C(15)	1705(2)	1349(2)	6327(2)	19(1)
C(16)	2011(2)	2803(2)	7195(2)	21(1)
C(17)	2827(2)	3853(2)	6840(2)	20(1)
C(18)	3331(2)	3441(2)	5603(2)	18(1)
Cl(1)	2933(1)	4003(1)	2426(1)	31(1)
Cl(2)	2871(1)	1488(1)	79(1)	27(1)

[a] U(eq) is defined as one-third of the trace of the orthogonalized U^{ij} tensor.

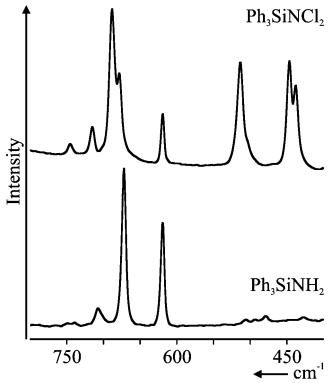

Figure 2. Raman spectra of Ph_3SiNCl_2 (upper) and Ph_3SiNH_2 (lower trace).

(33) Curtiss, L. A.; Raghavachari, K.; Redfern, P. C.; Pople, J. A. *J. Chem. Phys.* **1997**, *106*, 1063.

(34) Minkwitz, R.; Garzarek, P.; Preut, H. *Z. Naturforsch.* **1997**, *52b*, 88.

(35) Minkwitz, R.; Garzarek, P.; Neikes, F.; Kornath, A.; Preut, H. *Z. Anorg. Allg. Chem.* **1997**, *623*, 333.

Table 4. ^{1}H, ^{13}C, ^{29}Si, and ^{14}N NMR Spectra of *t*-$BuMe_2SiNCl_2$

		δ	$\Delta\nu_{1/2}$ (Hz)
^{1}H	$C(CH)_3$	2.25 (s)	
	$(CH_3)_2$	1.53 (s)	
^{13}C	$C(CH)_3$	27.15 (s)	
	$C(CH)_3$	19.96 (s)	
	$(CH_3)_2$	5.81 (s)	
^{29}Si		39.8 (s)	
^{14}N		−280 (s)	770

product (Figure 2) demonstrates that, upon chlorination, very intense, new bands at 688, 513, 446, and 437 cm^{-1} appear in the region of the $SiNCl_2$ stretching vibrations. On the basis of our theoretical calculations and normal coordinate analysis, these skeletal modes are strongly mixed. The 688 cm^{-1} mode is a mixture of Si−N and antisymmetric NCl_2 stretching and the 513 and 446/437 cm^{-1} modes are out-of-phase and in-phase combinations, respectively, of Si−N and symmetric NCl_2 stretching. For the highly characteristic NCl_2 vibrations, the expected frequency separation between antisymmetric and symmetric NCl_2 stretching would be much smaller and be on the order of 20−40 cm^{-1}.

Synthesis and Properties of *t*-$BuMe_2SiNCl_2$. Since our repeated efforts to duplicate the reported[15] preparation of trimethylsilyldichloramine failed, and the corresponding triphenylsilyl compounds were not volatile enough for our purposes, the previously unknown *tert*-butyl-dimethylsilyl-dichloramine was prepared according to eq 4.

$$t\text{-}BuMe_2SiNH_2 + 2t\text{-}BuOCl \xrightarrow{Et_2O} t\text{-}BuMe_2SiNCl_2 + 2t\text{-}BuOH \quad (4)$$

Unfortunately, the volatility of the dichloramine is similar to that of the byproduct *t*-BuOH, rendering the separation of the two compounds difficult and resulting in low isolated yields. At room-temperature, the moisture sensitive *t*-$BuMe_2SiNCl_2$ is a tacky yellow solid with a very intense odor and a melting point of ∼25−30 °C. It cannot be distilled without decomposition. Storage for a prolonged period of time at RT, especially under the influence of light, resulted in the formation of *t*-$BuMe_2SiCl$. Its purity was determined by Raman and NMR spectroscopy. The ^{1}H, ^{13}C, ^{29}Si, and ^{14}N NMR spectroscopic data of neat *t*-$BuMe_2SiNCl_2$ are listed in Table 4. The ^{1}H, ^{13}C, and ^{29}Si NMR chemical shifts are located in the region expected for the *t*-$BuMe_2Si$ group. The broad ^{14}N resonance for $-NCl_2$ at −280 ppm ($\Delta\nu_{1/2}$ = 770 Hz) lies within expectation.[36]

The Raman spectra of *t*-$BuMe_2SiNCl_2$ (upper) and of *t*-$BuMe_2SiNH_2$ (lower trace) are shown in Figure 3. While the *t*-$BuMe_2Si$-skeleton results again in complex vibrational spectra, a comparison of the two spectra reveals, for the NCl_2 compound, strong Raman bands at 676, 463, and 438 cm^{-1}. These are attributed, similar to those of Ph_3SiNCl_2, to NCl_2 motions which are strongly coupled to the skeletal C_3Si-N modes. In support of this interpretation, a normal coordinate analysis was carried out for the most simple, but unknown, silyldichloramine, H_3SiNCl_2. The calculated structure is shown in Figure 4, and the results from the normal coordinate analysis are summarized in Table 5. It can be seen from the potential energy distribution that, even in this relatively simple molecule, the skeletal modes are strongly mixed. For

(36) Wrackmeyer, B. *Spectrochim. Acta.* **1987**, *43*, 1187.

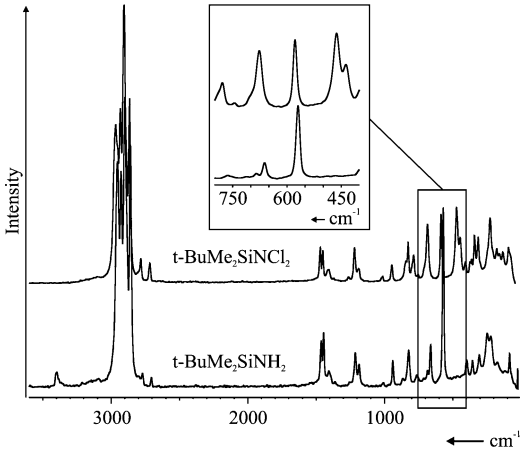

Figure 3. Raman spectrum of *t*-$BuMe_2SiNCl_2$ (upper) and *t*-$BuMe_2SiNH_2$ (lower trace).

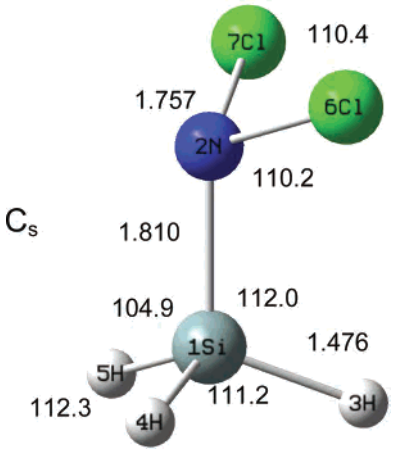

Figure 4. Geometry of H_3SiNCl_2, calculated at the MP2/6-31G(d) level (bond lengths in Å, angles in deg).

Table 5. Vibrational Frequencies (cm^{-1}), Calculated at the MP2/6-31G(d) Level, of H_3SiNCl_2 with C_s Symmetry, and Mode Description Derived from a Normal Coordinate Analysis

symmetry coordinate	calcd frequency	potential-energy distribution (%)
S1 ν sym SiH_3 in-phase	a′ ν_1 2362	88(1), 12(2)
S2 ν sym SiH_3 out-of-phase	ν_2 2331	89(2), 10(1)
S3 δ umbrella SiH_3	ν_3 988	54(4), 46(3)
S4 δ sciss SiH_2	ν_4 973	98(4)
S5 ν SiN	ν_5 883	55(5), 28(7), 12(9), 5(8)
S6 δ rock SiH_3	ν_6 703	96(6), 2(8), 1(9)
S7 ν sym NCl_2	ν_7 485	38(7), 25(5), 22(8), 11(9), 3(6)
S8 δ sciss NCl_2	ν_8 299	89(8), 5(6), 3(9), 2(5)
S9 δ Si-N═Cl_2	ν_9 206	67(9), 24(8), 6(6), 1(7)
S10 ν asym SiH_3	a″ ν_{100} 2375	100(10)
S11 δ as SiH_3	ν_{11} 995	63(11), 35(15)
S12 ν asym NCl_2	n_{12} 779	43(13), 29(15)(5), 18(12), 9(14)
S13 δ wag SiH_3	ν_{13} 653	81(13), 10(12), 7(15), 1(14)
S14 δ twist NCl_2	ν_{14} 218	92(15), 7(14)
S15 τ Si−N	ν_{15} 171	89(15), 10(14)

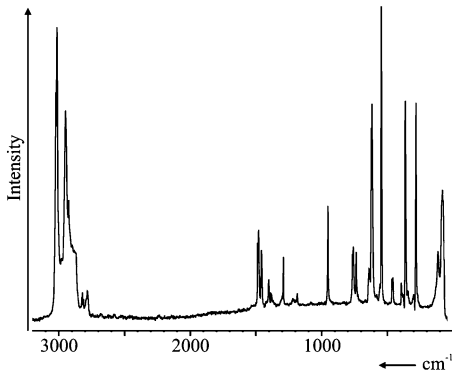

Figure 5. Raman spectrum of solid $Me_4NCl \cdot 1/3(NCl_3)$.

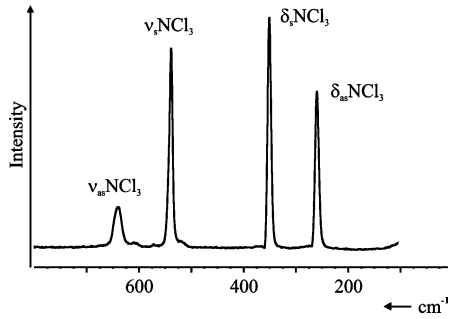

Figure 6. Raman spectrum of neat NCl_3.

example, the maximum contribution from symmetric NCl_2 stretching (S7) to any single mode does not exceed 38% and that from antisymmetric NCl_2 stretching (S12) is even smaller with 18%. This analysis demonstrates the fallacy of assigning, for these compounds, characteristic NCl_2 bands.

Reaction of *t*-BuMe$_2$SiNCl$_2$ with Tetramethylammoniumfluoride. The cleavage of the Si−N bond in *t*-BuMe$_2$SiNCl$_2$ by Me_4NF (eq 2) was studied in CHF_3 solution[16] at −78 °C. The solvent and the generated N_2 were pumped off at this temperature, and the *t*-BuMe$_2$SiF byproduct, which was formed in quantitative yield, was removed at −25 °C. The latter was identified by mass balance and IR, Raman, and NMR spectroscopy. The low-temperature Raman spectrum (Figure 5) of the solid residue showed bands from Me_4NCl and intense new bands at 635, 617, 611, 540, 356, and 276 cm^{-1}. Clearly, the number and frequencies of these bands were incompatible with the presence of an NCl_2^- anion which, on the basis of our theoretical predictions at the CCSD(T)/cc-pVTZ level, should exhibit only three bands with frequencies of 564, 517, and 255 cm^{-1}. The identity of the species, absorbed on the Me_4NCl, was established by warming the solid to room temperature and collecting the volatiles at −196 °C. On the basis of their Raman spectra, the solid residue consisted of Me_4NCl, while the volatile product, a yellow liquid at room temperature, was pure NCl_3.[37−40] Our Raman spectrum of liquid NCl_3 (Figure 6) is the first well-defined spectrum of the neat substance. Previously, only a partial spectrum of poor quality had been reported by Hendra and Mackenzie.[38] All these Raman data together with their assignments are listed in Table 6. To clarify the composition of the species absorbed on Me_4NCl at −25 °C, the collected NCl_3 was condensed back onto the Me_4NCl, and the low-temperature Raman spectrum was rerecorded. The spectrum was identical to the initial one, and this shows that the absorbed species is indeed NCl_3 and that its absorption and desorption are reversible. The marked differences in the spectra of absorbed and neat NCl_3 are attributed to crystal splittings and solid-state effects.

Table 6. Raman Spectra of Solid Me_4NCl, $Me_4NCl \cdot 1/3(NCl_3)$ and Neat Liquid NCl_3

Me_4NCl at RT		$Me_4NCl \cdot NCl_3$ at −25 °C		NCl_3 at RT		assignments	
						Me_4N^{+a}	NCl_3
3026	(95)	3026	(51)				
3018	(100)	3017	(71)				
2950	(83)	2952	(51)				
		2926	(31)				
		2898	(18)				
2877	(30)	2877	(15)			νCH_3 and combination bands	
		2827	(6)				
		2821	(7)				
		2813	(5)				
2788	(14)	2786	(7)				
1482	(32)	1483	(21)			ν_{15}	
1477	(30)	1477	(24)			ν_6	
1455	(15)	1455	(22)			ν_2	
1401	(13)	1399	(7)			ν_{16}	
1287	(13)	1288	(15)			ν_{17}	
1191	(1)	1191	(2)			ν_7	
1181	(5)	1181	(5)			ν_{11}	
948	(36)	947	(27)			ν_{18}	
803	(1)						
759	(29)	753	(16)			ν_3	
		732	(5)[b]				
		635	(11)				$\nu_2 + \nu_4$ (b_2)[c]
		617	(49)	640	(19)		ν_3 (b_2)[c]
		611	(61)				
565	(3)						
		550	(6)				
		540	(100)	539	(86)		ν_1 (a_1)
458	(13)	458	(7)			ν_{19}	
		452	(7)				
388	(5)	387	(5)			ν_8	
375	(3)	372	(5)			ν_8 or ν_{12}	
360	(3)						
		356	(70)	351	(100)		ν_2 (a_1)
		338	(5)				
		276	(61)	260	(69)		ν_4 (b_2)
109	(1)	108	(15)				
85	(9)						

[a] Based on refs 15 and 39. [b] Teflon−FEP band from the sample container. [c] Fermi resonance.

A plausible explanation for the overall process which led to the formation of Me_4NCl and NCl_3 is given by the following mechanism

$$t\text{-BuMe}_2\text{SiNCl}_2 + [\text{Me}_4\text{N}]^+\text{F}^- \rightarrow [\text{Me}_4\text{N}]^+[\text{NCl}_2]^- + t\text{-BuMe}_2\text{SiF} \quad (5)$$

$$[\text{Me}_4\text{N}]^+[\text{NCl}_2]^- \rightarrow \text{Me}_4\text{NCl} + \text{NCl} \quad (6)$$

$$2\text{NCl} \rightarrow \text{N}_2\text{Cl}_2 \quad (7)$$

$$3\text{N}_2\text{Cl}_2 \rightarrow 2\text{NCl}_3 + 2\text{N}_2 \quad (8)$$

$$3t\text{-BuMe}_2\text{SiNCl}_2 + 3\text{Me}_4\text{NF} \rightarrow 3\text{Me}_4\text{NCl} + \text{NCl}_3 + \text{N}_2 + 3t\text{-BuMe}_2\text{SiF} \quad (9)$$

The proposed mechanism is supported by the following theoretical calculations.

(37) Moore, G. E.; Badger, R. M. *J. Am. Chem. Soc.* **1952**, *74*, 6076.
(38) Hendra, P. J.; Mackenzie, J. R. *Chem. Commun.* **1968**, 760.
(39) Bayersdorfer, L.; Engelhardt, U.; Fischer, J.; Hoehne, K.; Jander, J. *Z. Anorg. Allg. Chem.* **1969**, *366*, 169.
(40) Gilbert, J. V.; Smith, L. J. *J. Phys. Chem.* **1991**, *95*, 7278.

Table 7. Optimized CCSD(T) Bond Lengths (Å) and Angles (deg) for N_xCl_y

molecule	basis set	R_{NN}	R_{NCl}	∠NNCl	∠ClNCl
NCl ($^3\Sigma^-$)	aV(D+d)Z		1.6556		
	aV(T+d)Z		1.6396		
	aV(Q+d)Z		1.6208		
NCl (^{1}D)	aV(D+d)Z		1.6146		
	aV(T+d)Z		1.5972		
	aV(Q+d)Z		1.5836		
NCl_2^-	aV(D+d)Z		1.8513		105.8
	aV(T+d)Z		1.8273		105.5
cis-N_2Cl_2	aV(D+d)Z	1.2204	1.8143	121.4	
	aV(T+d)Z	1.2130	1.7947	121.1	
trans-N_2Cl_2	aV(D+d)Z	1.2394	1.8027	107.6	
	aV(T+d)Z	1.2304	1.7847	107.8	

Stability Calculations for NCl_2^-. Although the NCl_2^- anion is predicted to be a minimum on the potential energy surface, its energy barrier toward the loss of a chloride ion could be low. NCl_2^- has a $^1A_1$ ground state. Breaking an N−Cl bond leading to the formation of ground state $^3\Sigma^-$ NCl and the ^{1}S Cl^- ion would require the least amount of energy but is spin-forbidden (eq 10).

$$NCl_2^- \rightarrow (^3\Sigma^-)\ NCl + Cl^- \qquad (10)$$

The lowest-energy spin-allowed pathway on the singlet potential energy surface leads to formation of excited state ($^1\Delta$) NCl (eq 11).

$$NCl_2^- \rightarrow (^1\Delta)\ NCl + Cl^- \qquad (11)$$

Thus for NCl_2^- to dissociate by the low-energy path to ground state products, a spin-forbidden process has to occur. In the simplest approximation, the barrier for a simple bond-dissociation step is given by the dissociation energy. Therefore, the energies for reactions 10 and 11 provide values for the minimum energy barriers. To obtain these values, we first calculated the properties of NCl and NCl_2^-. The geometries (Table 7), vibrational frequencies (Table 8), and energy components for the total atomization energies (Table 9) were calculated at the CCSD(T) level, and the corresponding heats of formation at 0 and 298 K are given in Table 10. The calculated total valence CCSD(T) energies as a function of basis set are given in Table 11.

The energy difference between ground state ($^3\Sigma^-$) NCl and excited state ($^1\Delta$) NCl is calculated to be 32.5 kcal/mol at 0 K, in good agreement with the lower level QCISD(T)/6-311++G(2df,p) calculations of Milburn et al.[43] who obtained 30.2 kcal/mol for this energy difference. The bond-dissociation energy to the ground state products is predicted to be 6.4 kcal/mol at 0 K and 7.1 kcal/mol at 298 K. The lowest bond-dissociation energy for spin-allowed products is predicted to be 38.9 kcal/mol at 0 K and 39.7 kcal/mol at 298 K. As a result of the entropy contribution, the value of the free-energy change, ΔG_r(298 K), for reaction 10 becomes negative (−0.6 kcal/mol). This shows that, at room temperature, the spontaneous loss of Cl^- with simultaneous formation of ground state ($^3\Sigma^-$) NCl would be thermodynamically allowed. Our calculated bond-dissociation enthalpy values of 6.4 and 38.9 kcal/mol for reactions 10 and 11, respectively, are in good agreement with those of 7.3 and 37.5 kcal/mol by Milburn et al.[43]

As already stated above, a spin crossing must occur for NCl_2^- to dissociate along the spin-forbidden low-energy path (10). To determine if there is a low-lying intersection between the potential curves of ground state ($^3\Sigma^-$) NCl and excited state ($^1\Delta$) NCl, which could lower this barrier, full valence complete active space self-consistent field (CASSCF) calculations[41] with the 6-311+G(2df) basis set[42] were performed to map out the lowest dissociative singlet and triplet potential-energy surfaces and to determine the point at which they intersect. These calculations, which include nondynamical correlation but omit dynamical correlation effects, show that formation of excited ($^1\Delta$) NCl plus chloride and that of ground state ($^3\Sigma^-$) NCl plus chloride differ by 31.6 kcal/mol, in good agreement with our CCSD(T)/CBS value of 32.5 kcal/mol. The point where the lowest singlet and triplet potential-energy surfaces intersect corresponds to a partially dissociated NCl_2^- species with N−Cl bond distances of 1.727 and 2.177 Å and a Cl−N−Cl bond angle of 105.6° and is 6.9 kcal/mol higher in energy than the NCl_2^- local minimum. These geometry parameters were used as input for single-point CCSD(T) calculations of the singlet and triplet energies. The CCSD(T)/CBS-limit results give a singlet−triplet splitting of 4.2 kcal/mol and, at this geometry, the singlet and triplet are 9.1 and 13.3 kcal/mol, respectively, above the ground state of NCl_2^-. The singlet−triplet splitting varies with the basis set. For example, the CCSD(T)/aug-cc-pV(D+d)Z value is 0.7 kcal/mol, whereas the CCSD(T)/aug-cc-pV(T+d)Z value is 1.4 kcal/mol. Further single-point calculations at the CCSD(T)/aug-cc-pV(Q+d)Z level show that the singlet−triplet crossing occurs between 2.2 and 2.25 Å for the longer N−Cl distance, with 1.7 Å for the shorter N−Cl bond distance and the same bond angle as given above. This is consistent with the CASSCF results. *Thus, the intersystem crossing region occurs at essentially the same energy as the final dissociation energy to the ground state products. If there is sufficient spin−orbit coupling in the vicinity of the intersection, intersystem crossing from the initial singlet state to the triplet electronic state will occur, and there is essentially no barrier other than the endothermicity of the process.*

Stability Calculations for N_2Cl_2. Out of the three possible isomers of N_2Cl_2, only the cis and the trans isomers are vibrationally stable, while the iso isomer is not a minimum on the potential-energy surface (Figure 7). As has been

(41) The NCl_2^- full valence CASSCF wavefunction is a linear combination of configurations generated by distributing the 20 valence electrons among the 12 valence orbitals in all possible ways which are consistent with the overall space and spin symmetry of the molecular electronic state. For example, see: (a) Schmidt, M. W.; Gordon, M. S. *Ann. Rev. Phys. Chem.* **1998**, *49*, 233. (b) Roos, B. O. In *Methods in Computational Molecular Physics*; Diercksen, G. H. F.; Wilson, S., Eds.; D. Riedel Publishing: Dordrecht, The Netherlands, 1983; pp 161−187.

(42) (a) Krishnan, R.; Binkley, J. S.; Seeger, R.; Pople, J. A. *J. Chem. Phys.* **1980**, *72*, 650−654. (b) Frisch, M. J.; Pople, J. A.; Binkley, J. S. *J. Chem. Phys.* **1984**, *80*, 3265. (c) Clark, T.; Chandrasekhar, J.; Spitznagel, G. W.; von Ragué Schleyer, P. *J. Comput. Chem.* **1983**, *4*, 294.

(43) Milburn, R. K.; Rodriquez, C. F.; Hopkinson, A. C. *J. Phys. Chem. B* **1997**, *101*, 1837.

Table 8. Calculated Vibrational Frequencies (cm^{-1})

symmetry	ν MP2/6-311+G(d)	ν CCSD(T)/cc-pVTZ[a]	I (IR)[b] MP2/6-311+G(d)	I (IR)[a,b] CCSD(T)/cc-pVTZ	I (Raman)[c] MP2/6-311+G(d)
NCl ($^3\Sigma^-$)[d]	ω_e ($\omega_e x_e$)	1162.8 (12.7)			
NCl ($^1\Delta$)[d]	ω_e ($\omega_e x_e$)	1286.5 (10.7)			
NCl_2^-					
a_1	601.4	579.3/563.9	0.5	1.4	10.2
	270.9	257.9/255.2	2.3	2.1	10.3
b_2	599.4	525.6/517.3	78.7	89.2	25.5
NCl_3					
a_1	372.4	354.2	0.2	0.2	12.4
	540.6	550.7	0	0.02	10.4
e	271.0	261.8	0.5	0.4	6.0
	685.9	673.6	53.4	53.6	5.3
NCl_4^+					
a_1	442.6	448.6	0	0	17.8
e	223.0	216.4	0	0	3.9
t_2	316.3	304.4	0.2	0.2	6.3
	723.1	733.8	20.8	17.6	2.7
cis-N-$_2Cl_2$					
a_1	1518.3	1580.4/1585.2	100.0	83.0/78.9	191.2
	501.4	531.6/531.0	35.6	28.1/26.3	41.6
	197.6	203.8/206.7	1.94	1.1/1.2	17.7
a_2	454.6	347.5/462.8	0	0/0	0
b_2	722.0	880.6/722.1	130.3	157.0/139.1	0.8
	387.8	536.3/423.5	186.7	16.0/136.5	29.5
trans-N-$_2Cl_2$-					
a_g	1438.4	1530.1/1537.6	0	0/0	139.7
	814.4	787.0/790.1	0	0/0	33.8
	335.6	320.4/326.6	0	0/0	45.0
a_u	232.6	472.6/229.9	0.1	0.3/0.1	0
b_u	656.8	740.5/638.9	178.3	568.4/182.8	0
	283.2	251.0/276.6	3.1	99.8/3.4	0
N_2Cl_4					
a_g	745.2		0		5.0
	687.4		0		22.0
	374.9		0		22.1
	255.5		0		2.5
b_g	808.8		0		15.2
	300.1		0		10.6
a_u	688.1		1.5		0
	200.5		0.0		0
	63.9		0.0		0
b_u	621.7		0.7		0
	336.5		0.0		0
	310.8		0.0		0

[a] Values after a slash are with the aug-cc-pVTZ basis set. [b] Infrared intensity in km mol^{-1}. [c] Raman intensity in $Å^4$ amu^{-1} [d] Diatomic molecule frequencies, ω_e, calculated with the aug-cc-pV(Q+d)Z level with a fifth-order fit. $\omega_e x_e$ is given in parentheses.

Table 9. Components for Calculated Atomization Energies (kcal mol^{-1})

molecule	CBS[a]	ΔE_{ZPE}[b]	ΔE_{CV}[c]	ΔE_{SR}[d]	ΔE_{SO}[e]	ΣD_0 (0 K)[f]
Cl^-	84.70	0.00	0.04	0.74	−0.84	84.64
NCl ($^3\Sigma^-$)	66.81	1.65	0.21	0.92	−0.84	65.45
NCl ($^1\Delta$)	34.62	1.83	0.03	0.91	−0.84	32.89
NCl_2^-	158.22	1.91	0.22	1.63	−1.68	156.48
cis-N_2Cl_2	229.64	5.62	0.59	1.78	−1.68	224.71
trans-N_2Cl_2	225.80	5.43	0.61	1.75	−1.68	221.05

[a] Extrapolated by using eq 1 with aug-cc-PV(n+d)Z, $n = D, T, Q$. [b] The zero-point energies were obtained as described in the text. [c] Core/valence corrections were obtained with the cc-pwCVTZ basis sets at the optimized geometries. [d] The scalar relativistic correction is based on a CISD(FC)/cc-pVTZ MVD calculation. [e] Correction from the incorrect treatment of the atomic asymptotes as an average of spin multiplets. Values are based on *C*. Moore's Tables, ref 45. [f] The theoretical value of the dissociation energy to atoms ΣD_0 (0 K).

shown in a previous high-level study by Tschumper, Heaven, and Morokuma,[44] the cis and the trans isomers of N_2Cl_2 also have very low predicted barriers to dissociation of only 7−8 kcal/mol at the CCSD(T) level and of ≤1.5 kcal/mol at the CASPT2 (complete active space with second-order perturbation theory) level and are weakly bound. We also calculated the heat of formation of *cis*- and *trans*-N_2Cl_2 using our additive CCSD(T)/CBS (coupled cluster/complete basis set) approach. The cis isomer is more stable than the trans isomer by 3.8 kcal/mol at 298 K, consistent with the electronic energy difference of 4.0 kcal/mol reported by Tschumper et al.[44] The energies for reactions 12 and 13, using the experimental heats of formation for Cl and N_2 (at this level of calculation, there is an error of 0.8 kcal/mol in the bond

Table 10. Heats of Formation (kcal mol^{-1}) at 0 and 298 K

molecule	ΔH_f(0 K)$_{theory}$	ΔH_f(298 K)$_{theory}$
Cl^-	−56.1	−55.7
NCl ($^3\Sigma^-$)	75.7	75.6
NCl ($^1\Delta$)	108.2	108.2
NCl_2^-	13.2	12.8
cis-N_2Cl_2	57.5	56.5
trans-N_2Cl_2	61.2	60.3

(44) Tschumper, G. S.; Heaven, M. C.; Morokuma, K. *Chem. Phys. Lett.* **2003**, *370*, 418.

Table 11. Total CCSD(T) Energies (E_h) as a Function of Basis Set

system	basis set	E_h
Cl^-	aVDZ	−459.743800
	aVTZ	−459.806626
	aVQZ	−459.828395
	CBS	−459.840937
NCl ($^3\Sigma^-$)	aVDZ	−514.187359
	aVTZ	−514.274307
	aVQZ	−514.316784
	CBS	−514.342499
NCl ($^1\Delta$)	aVDZ	−514.128403
	aVTZ	−514.216831
	aVQZ	−514.263024
	CBS	−514.291207
NCl_2^-	aVDZ	−973.930708
	aVTZ	−974.084038
	aVQZ	−974.152887
	CBS	−974.194135
cis-N_2Cl_2	aVDZ	−1028.514405
	aVTZ	−1028.687711
	aVQZ	−1028.780956
	CBS	−1028.838016
trans-N_2Cl_2	aVDZ	−1028.508695
	aVTZ	−1028.682210
	aVQZ	−1028.775094
	CBS	−1028.831905

energy of N_2) are predicted to be 94.8 and 1.6 kcal/mol,

$$cis\text{-}N_2Cl_2 \rightarrow 2NCl\ (^3\Sigma^-) \quad (12)$$

$$cis\text{-}N_2Cl_2 \rightarrow N_2 + 2Cl \quad (13)$$

respectively. The former value is in good agreement with that predicted by Tschumper et al.,[44] but the latter value is substantially different from their reported value of −21 kcal/mol obtained with a smaller basis set. (The reported value is in error and this value should be −9.6 kcal/mol.) Tschumper et al.[44] calculated the transition state for dissociation for reaction 13 at the CCSD(T) and 8e/8o-CASPT2 levels with a TZ2P(f) basis set and found the geometries to be similar. We used their CCSD(T) geometries and obtained a barrier of 10.8 kcal/mol at the CCSD(T)/CBS limit, consistent with their value of 7.3 kcal/mol at the CCSD(T)/TZ2P(f) level. The CCSD(T)/aug-cc-pV(T+d)Z value is 7.2 kcal/mol. The CASPT2 barrier is predicted to be much lower, 0.9 kcal/mol.

Using Tschumper et al.'s CCSD(T) geometry,[44] we found that the CCSD(T)/CBS barrier height for the decomposition of the trans isomer to N_2 + 2Cl is 11.5 kcal/mol, similar to their value of 7.9 kcal/mol at the CCSD(T)/TZ2P(f) level. The use of their CASPT2 geometry at the CCSD(T)/CBS limit resulted in a lower barrier height of 9.3 kcal/mol, but again, this is substantially higher than their 8e/8o-CASPT2 value of 1.5 kcal/mol. Thus, the N_2Cl_2 isomers are stable minima on the potential energy surfaces, but they possess low barriers to dissociation into diatomic N_2 and two Cl atoms. On the basis of the CASPT2 and CCSD(T) results, these barriers to dissociation lie between 1 and 11 kcal/mol. It should be noted that the value for the T_1 diagnostic, which serves as a measure for the reliability of results obtained from single-reference correlation procedures,[46] is not large for *cis*-N_2Cl_2 (0.0195) and is not that large even for the transition state (0.0243), suggesting that these molecules are dominated by a single reference configuration. *Therefore, our CCSD(T)/CBS values of 10.8 and 11.5 kcal/mol for the barriers of the decompositions of cis- and trans-N_2Cl_2, respectively, to N_2 and two Cl atoms should be relaible to 1 or 2 kcal/mol, and N_2Cl_2 should readily decompose under the experimental conditions used in our study.*

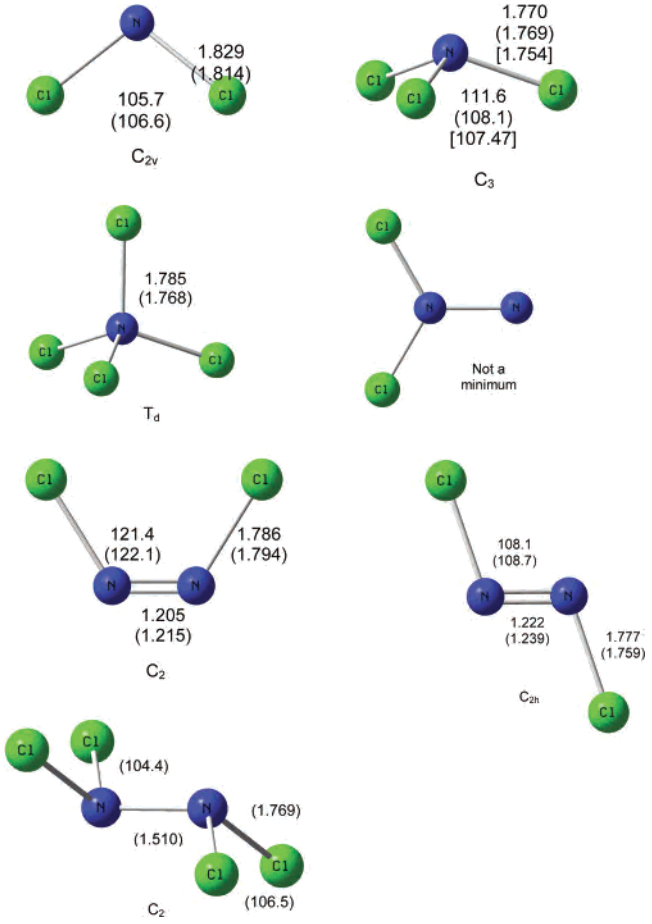

Figure 7. Calculated CCSD(T)/cc-pvtz geometries of NCl_2^-, NCl_3, NCl_4^+, *cis*-N_2Cl_2, *trans*-N_2Cl_2, *iso*-N_2Cl_2, and N_2Cl_4; the numbers in parantheses are the MP2/6-311+G(d) values and numbers in brackets are experimental values (bond lengths in Å, angles in deg).

Calculations for NCl_4^+, NCl_3 and N_2Cl_4. For comparison, we have also calculated the structures (Figure 7) and vibrational spectra (Table 8) of the NCl_4^+ and NCl_2^- ions and the *cis*-N_2Cl_2, *trans*-N_2Cl_2, N_2Cl_4, and NCl_3 molecules at the CCSD(T)/cc-pvtz and MP2/6-31+G(d) levels of theory. Whereas the agreement between the CCSD(T) and MP2 calculations was quite good for the geometries of all compounds and the vibrational frequencies of the relatively well bound NCl_3 and NCl_4^+ species, for the N_2Cl_2 isomers and NCl_2^-, there were larger discrepancies between the

(45) Moore, C. E. *Atomic Energy Levels as Derived from the Analysis of Optical Spectra*; U.S. National Bureau of Standards Circular 467; U.S. Department of Commerce, National Technical Information Service, Washington, DC, 1948; Vol. 1 (H to V), COM-72-50282.
(46) (a) Lee, T. J.; Rice, J. E.; Scuseria, G. E.; Schaefer, H. F. III. *Theor. Chim. Acta.* **1989**, *75*, 81. (b) Lee, T. J. *Chem. Phys. Lett.* **2003**, *372*, 362.

CCSD(T) and MP2 vibrational frequencies, indicating that the frequency predictions for these weakly bound species are difficult. For example, for NCl_2^-, the symmetric stretch and bend are in good agreement between the two methods but the antisymmetric stretch which corresponds to the dissociation channel is lower by about 80 cm^{-1} at the CCSD(T) level. In *cis*-N_2Cl_2, the biggest change is found in the comparison of the CCSD(T) triple-ζ calculations with and without diffuse functions. The MP2/6-311+G(d) and CCSD(T)/aug-cc-pVTZ results are in quite good agreement, whereas the CCSD(T)/cc-pVTZ results differ especially for the a_2 and b_2 modes with much higher frequencies for these modes. This could be because species near transition states (weakly bonded molecules) often require diffuse functions for their proper characterization. For both *cis*- and *trans*-N_2Cl_2, the CCSD(T) method predicts a stronger N−N bond than does the MP2 method. For *trans*-N_2Cl_2, the CCSD(T)/cc-pVTZ calculations behave similar to those for the cis isomer with substantial differences found for the a_u and highest b_u modes as compared to the MP2 and CCSD(T) calculations with diffuse functions in the basis set.

Conclusions

Only two silyldichloramines, $(CH_3)_3SiNCl_2$ and $(C_6H_5)_3SiNCl_2$, had previously been reported. Out of these, only the synthesis of $(C_6H_5)_3SiNCl_2$ could be duplicated, and its crystal structure was determined. The new silyldichloramine, *t*-$BuMe_2SiNCl_2$, was prepared and characterized. It is shown that, in these triorganylsilyldichloramines and the yet unknown H_3SiNCl_2, the NCl_2 stretching modes strongly couple to the skeletal modes, thus making it impossible to assign characteristic stretching frequencies to the NCl_2 group. The reaction of *t*-$BuMe_2SiNCl_2$ with $[N(CH_3)_4]^+F^-$ provides indirect evidence for the formation of the unstable intermediates $[N(CH_3)_4]^+NCl_2^-$ and N_2Cl_2, giving rise to $[N(CH_3)_4]^+Cl^-$ and NCl_3 as the final products. The latter two compounds reversibly form a loose adduct, exhibiting a Raman spectrum which deviates significantly from that of pure NCl_3. Also, a reliable Raman spectrum of highly explosive, neat liquid NCl_3 has been recorded for the first time. Theoretical calculations for NCl_2^-, NCl_3, N_2Cl_4, NCl_4^+, and the different isomers of N_2Cl_2, strongly support the inferred instabilities of NCl_2^- and N_2Cl_2 and demonstrate the difficulties involved in making reliable stability and property predictions for very weakly bound systems.

Acknowledgment. The authors thank the National Science Foundation, the Air Force Office of Scientific Research, and the Office of Naval Research for financial support. We thank Prof. G. A. Olah and the Loker Research Institute for their steady support and hospitality and Irina Tsyba for her help with the crystal structure determination. This paper is dedicated to our friend and esteemed colleague, Prof. William P. Weber, on the occasion of his retirement.

IC0609103